

## Breakup Densities of Hot Nuclei

V. E. Viola

*Department of Chemistry and IUCF, Indiana University, Bloomington, Indiana 47405, USA*

K. Kwiatkowski

*Physics Division, Los Alamos National Laboratory, Los Alamos, New Mexico 87545, USA*

J. B. Natowitz and S. J. Yennello

*Department of Chemistry and Cyclotron Institute, Texas A&M University, College Station, Texas 77843, USA*

(Received 11 March 2004; published 21 September 2004)

Breakup densities of hot  $^{197}\text{Au}$ -like residues have been deduced from the systematic trends of Coulomb parameters required to fit intermediate-mass-fragment kinetic-energy spectra. The results indicate emission from nuclei near normal nuclear density below an excitation energy  $E^*/A \lesssim 2$  MeV, followed by a gradual decrease to a near-constant value of  $\rho/\rho_0 \sim 0.3$  for  $E^*/A \gtrsim 5$  MeV. Temperatures derived from these data with a density-dependent Fermi-gas model yield a nuclear caloric curve that is generally consistent with those derived from isotope ratios.

DOI: 10.1103/PhysRevLett.93.132701

PACS numbers: 25.70.Pq, 25.55.-e

Knowledge of the dependence of nuclear density on excitation energy is of central importance in understanding nuclear compressibility and the equation of state of finite nuclear matter. The breakup density is particularly relevant to models of multifragmentation phenomena [1–4], which assume that at sufficiently high temperatures thermal pressure and Coulomb forces drive nuclear expansion and subsequent decomposition of the system. The models of Refs. [1–3] assume an *a priori* breakup density,  $\rho/\rho_0$ , when the threshold temperature for multifragmentation is reached; i.e., the transition can be viewed as abrupt. In the models of Refs. [4,5], the breakup density decreases continuously as a function of excitation energy. This transition from normal to dilute nuclear density depends upon the stiffness of nuclear matter as a function of temperature. Hence, it is important to obtain experimental data that relate the breakup density to the temperature of the fragmenting source.

Previous experimental studies [6] have shown that, above an excitation of about 4 MeV per nucleon, the breakup time scale is of order 20–50 fm/c. In this same excitation-energy region, derived nuclear temperatures deviate significantly from Fermi-gas expectations and caloric-curve-like behavior is observed [7]. Here we extract breakup densities from experimental intermediate-mass-fragment (IMF) spectra and examine the results in the context of current nuclear caloric-curve results.

Perhaps the most direct experimental signal of decreasing nuclear density is found in the centroids of the Coulomb-like peaks of the kinetic-energy spectra for intermediate-mass fragments (IMF:  $3 \leq Z \leq 15$ ) produced in thermal-like events. The peak centroids are expected to increase systematically with increasing excitation energy due to combined Coulomb and temperature effects. Experimentally, just the opposite is observed at

high excitation energy per nucleon  $E^*/A$  [8–10], which suggests emission from an expanded/dilute source.

Recently, the density evolution as a function of excitation energy has been derived from caloric-curve measurements [11]. In this analysis, the inverse level-density parameter,  $K(\rho)$ , is given by

$$K(\rho) = \frac{T^2}{(\varepsilon_{th})} \left( \frac{\rho}{\rho_0} \right)^{2/3} \left( \frac{m^*(\rho_0)}{m^*(\rho)} \right), \quad (1)$$

where  $\varepsilon_{th}$  is the thermal energy per nucleon,  $m^*$  is the effective nucleon mass,  $\rho_0$  is the central density of normal nuclear matter, and the temperature  $T$  is derived from double-isotope ratios [12]. From the caloric-curve data, the corresponding density can be derived. The results [11] indicated a decreasing density from unity at low excitation energies to  $\rho/\rho_0 \approx 0.40$  near  $E^*/A \approx 6$ –7 MeV, followed by a near-constant density at higher  $E^*/A$ .

In this Letter, we use experimental data based on IMF kinetic-energy spectra to determine the breakup density as a function of excitation energy. As an initial approximation, we assume that the effective mass ratio is unity and  $\varepsilon_{th}$  can be approximated by the excitation energy per nucleon obtained from calorimetry,  $E^*/A$ . Then the ratio  $K(\rho)/K_0$  becomes

$$K(\rho) = K_0(\rho/\rho_0)^{2/3} = T^2/(E^*/A). \quad (2)$$

Thus, temperatures derived from density information are independent of those derived from isotope ratios. The analysis employs three data sets spanning the excitation-energy range  $E^*/A = 0.9$  to 7.9 MeV: inclusive 200 MeV  $^4\text{He} + ^{197}\text{Au}$  [13] and (20–100)A MeV  $^{14}\text{N} + ^{197}\text{Au}$  [14], and exclusive 4.8 GeV  $^3\text{He} + ^{197}\text{Au}$  reactions [15]. Each of these systems was measured with very low kinetic-energy thresholds for IMF identification and covered nearly the entire angular range.

Calculation of  $E^*/A$  for the inclusive reactions involved the following assumptions. For the 200 MeV  ${}^4\text{He}$  bombardments, complete fusion was assumed for events in which an IMF was emitted. For this system, moving-source velocities are consistent with full-momentum transfer. For the  ${}^{14}\text{N}$  projectile, data obtained at  $E/A = 20$  and 30 MeV behaved similarly to the 200 MeV  ${}^4\text{He}$  case, and source velocities were consistent with full-momentum transfer [14]. Fits to the  ${}^{14}\text{N}$ -induced data at  $E/A = 40, 50, 60, 80,$  and 100 MeV yielded source velocities systematically lower than the full-momentum-transfer value. For these cases, an incomplete-fusion model was assumed to account for this energy loss, using the equilibrium source velocity obtained from the fitting procedure (below). The  $E^*/A$  values for the 4.8 GeV  ${}^4\text{He}$  reaction were obtained from calorimetry, as described by Kwiatkowski *et al.* and Lefort *et al.* [16,17].

Representative IMF kinetic-energy spectra for  $Z = 6$  fragments are shown in Fig. 1 as a function of  $E^*/A$ , measured for the 4.8 GeV  ${}^3\text{He} + {}^{197}\text{Au}$  system. The decrease in the peak centroids with increasing bombarding energy and angle is evident. Spectra were analyzed in terms of a two-component (three for  ${}^{14}\text{N}$ ) moving-source parametrization [18]. These sources were (i) an equilibrium source described by the transition-state formalism adopted from Moretto [19,20], (ii) a nonequilibrium source which employed a standard Maxwellian distribution, and (iii) a projectile-fragmentation source for  ${}^{14}\text{N}$  breakup. Details are given in Refs. [13–15].

For present purposes, only the equilibrium source is relevant. The model parameters are  $d^2\sigma/d\Omega dE = f(Z_{\text{IMF}}, \beta, k_C, T, p)$ , where  $\beta$  is the source velocity ( $v/c$ ),  $T$  is the spectral slope temperature, and  $p$  accounts for Coulomb barrier fluctuations [18]. Of primary im-

portance, the parameter  $k_C$  is the fractional Coulomb barrier energy,  $k_C = B_C/B_{\text{fission}}$ .  $B_C$  is the mutual repulsion energy between the IMF and its heavy partner, given by  $B_C = 1.44 Z_{\text{IMF}}Z_{\text{residue}}/d$ , where  $d = d_0 (A_{\text{IMF}}^{1/3} + A_{\text{residue}}^{1/3})$ . For  $A \sim 160$ –180,  $d_0 \approx 1.80$ –1.90 fm when  $k_C = 1.00$ .  $B_{\text{fission}}$  is based upon fission fragment average kinetic-energy release systematics [21], which provide a good fit to IMF evaporation spectra at low energies, where emission from nuclei near normal density is expected.

In the analysis, average values  $\langle k_C \rangle$  were determined from fits to  $Z = 5$ –10 spectra for the 200 MeV  ${}^4\text{He} + {}^{197}\text{Au}$  systems [13],  $Z = 3$ –9 for the 4.8 GeV  ${}^3\text{He} + {}^{197}\text{Au}$  experiments [15], and  $Z = 3$ –15 for the  ${}^{14}\text{N} + {}^{197}\text{Au}$  studies [14]. Errors include both statistical and systematic effects. Values of  $\langle k_C \rangle$  are plotted as a function of excitation energy in the top panel of Fig. 2. To make the  ${}^3\text{He}$  and  ${}^{14}\text{N}$  data self-consistent, we have normalized the 4.8 GeV data at  $E^*/A = 3.4$  MeV to the  ${}^{14}\text{N}$  data at  $E^*/A = 3.30$  and 3.65 MeV (normalization factor of 0.98).

Breakup-density information resides in the Coulomb barrier parameter  $k_C$ . We assume that for these light-ion-induced reactions, the thermal source is spherical and the expansion is radial. Since the Coulomb barrier is inversely proportional to the separation distance  $d$  between the charge centers of the IMF and its source, the density ( $\rho \propto 1/d^3$ ) can be expressed as

$$\rho/\rho_0 = \left( \frac{B_C}{B_{\text{fission}}} \right)^3 = k_C^3. \quad (3)$$

In the bottom panel of Fig. 2, the average breakup densities  $\langle \rho/\rho_0 \rangle$  derived from the above assumptions are plotted as a function of excitation energy. Between  $E^*/A = 2$  and 5 MeV, the analysis indicates a systematic decrease in density from  $\rho/\rho_0 \approx 1.0$  to  $\rho/\rho_0 \approx 0.30$ . It is

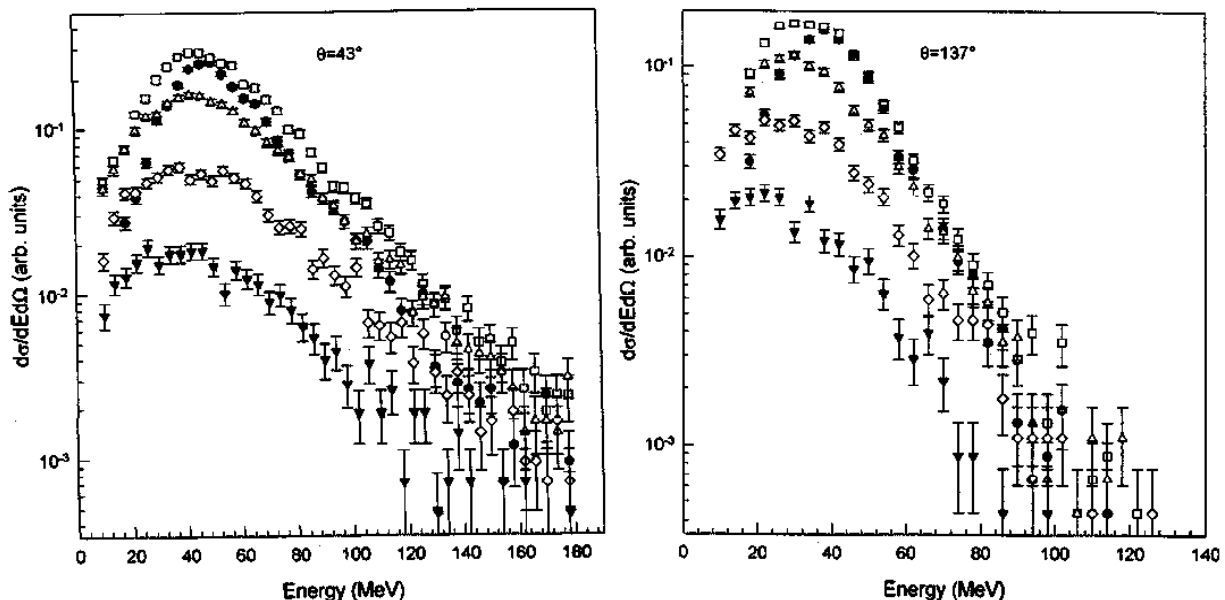


FIG. 1. Energy spectra at  $43^\circ$  and  $137^\circ$  for carbon fragments emitted from the 4.8 GeV/c  ${}^3\text{He} + {}^{197}\text{Au}$  reaction as a function of excitation energy. Symbols are as follows:  $\langle E^*/A \rangle = 3.4$  MeV ( $\bullet$ ); 4.6 MeV ( $\square$ ); 5.7 MeV ( $\triangle$ ); 6.8 MeV ( $\diamond$ ); 7.9 MeV ( $\blacktriangledown$ ).

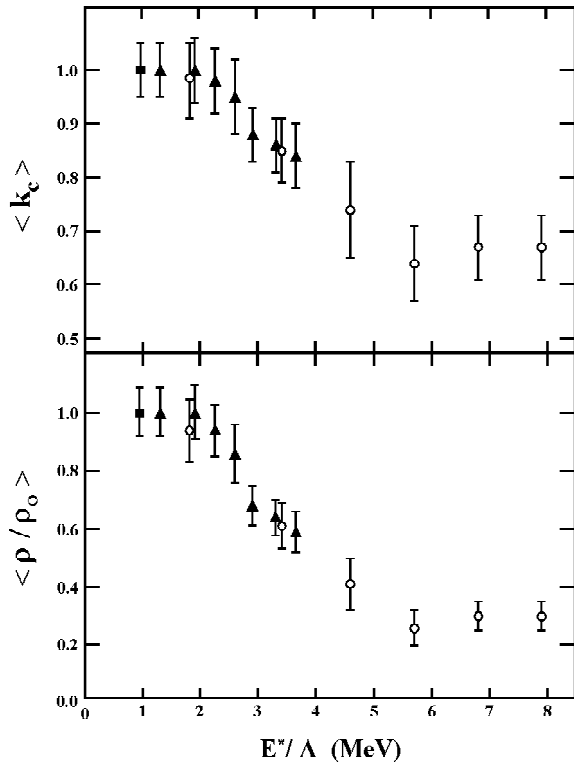


FIG. 2. Top: Dependence of the average moving-source Coulomb parameter  $\langle k_C \rangle$  as a function of excitation energy. Symbols are as follows: 200 MeV  ${}^4\text{He}$  (■);  ${}^{14}\text{N}$  (▲); 4.8 GeV  ${}^3\text{He}$  (○). Bottom: Average density  $\langle \rho/\rho_0 \rangle$  as a function of  $E^*/A$  derived from the  $k_C$  values in the top panel.

in this same range of excitation energies that 8.0 GeV/c  $\pi^- + {}^{197}\text{Au}$  exclusive studies show a rapid decrease in the emission time scale and a corresponding increase in multiple IMF production [22], as well as a distinct slope change in the caloric curve [23] and negative heat capacity [24]. Above  $E^*/A \geq 5$  MeV, a nearly constant value of  $\langle \rho/\rho_0 \rangle \approx 0.30$  is found. In this regard, it should be stressed that the fit procedure for the 4.8 GeV  ${}^3\text{He} + {}^{197}\text{Au}$  data [15] attempted to extract upper limits for the values of  $k_C$ , and correspondingly  $\rho/\rho_0$ . The relative constancy of  $\langle \rho/\rho_0 \rangle$  at high  $E^*/A$  suggests that the limiting density at which freeze-out occurs is reached near  $E^*/A \approx 5-6$  MeV for nuclei in this system [25,26].

Using the derived average densities, it is of interest to examine the density-dependent Fermi-gas temperatures [Eq. (2)] implied by these studies. When correlated with the corresponding excitation energies, this procedure generates a caloric curve for nuclei in the  $A \sim 150-190$  mass region (Fig. 3). In this analysis, we assume an empirical inverse level-density parameter of  $K_0 = 11.3$  MeV for normal nuclear density  $\rho_0$ , determined from a fit to the data below  $E^*/A = 2.0$  MeV. This gives  $T = \sqrt{11.3(\rho/\rho_0)^{2/3}(E^*/A)}$  MeV. Up to  $E^*/A = 2$  MeV, the temperature rises according to Fermi-gas predictions for normal nuclear density. In the region  $E^*/A =$

2–5 MeV, a distinct change in slope is observed for the data. Above  $E^*/A \approx 5$  MeV, a constant value of  $\rho/\rho_0 = 0.30$  in Eq. (2) yields a simple dependence on the square root of the excitation energy,  $T = 2.2\sqrt{(E^*/A)}$ . Overall, the results are strikingly similar to those obtained using the double-isotope-ratio thermometer [7,11], as well as with statistical multifragmentation model calculations that assume  $\rho/\rho_0 \approx 1/3$  at breakup [1–3].

We note, however, that the treatment that leads to the results presented in Fig. 3 makes two simplifying assumptions: (i) the excitation energy determined by the calorimetric technique is entirely thermal energy, and (ii) a single value for the inverse level-density parameter,  $K$ , is valid over the entire excitation-energy range sampled. Previous experimental and theoretical works have shown that the initial heating of the nucleus leads to a small expansion, the washing out of shell effects, and an increase in the nucleon effective mass, resulting in a decrease of the nuclear level density, reflected as an increase in the inverse level-density parameter,  $K$  [27–29]. Further, some of the available energy determined from calorimetry is required for expansion and thus is not available as intrinsic thermal energy. It is interesting therefore to attempt a second-order treatment in which these effects are taken into consideration.

In Ref. [11], the Fermi energy determinations of Moniz *et al.* [30] were employed to determine the appropriate reference value of  $K_0$ , i.e., the value expected when the shell effects and collective effects leading to increased level density above that predicted by the Fermi-gas model are no longer important and the effective mass  $m^* \sim 1$ . For the mass region sampled in the present experiments, the measurements of Ref. [30] indicate  $K_0 \sim 15.2$ . Data such as those in Fig. 1 of Ref. [11] indicate that such values are reached at  $\sim 2.5$  MeV per nucleon excitation energy. For the following, we assume a linear increase of  $K$  from 8 to  $\sim 15$  in the excitation-energy range of 1 to

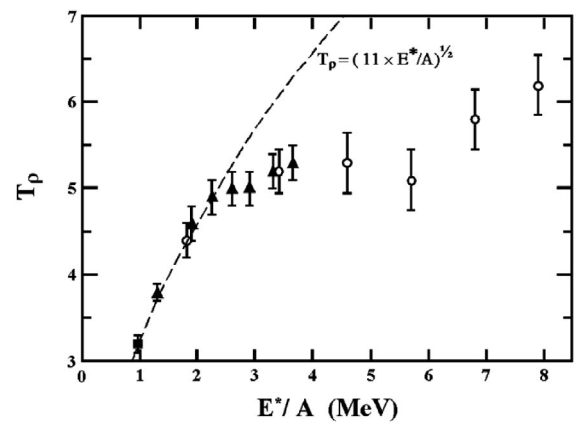


FIG. 3. First-order density-dependent Fermi-gas temperatures as a function of excitation energy. The dashed line is the normal-density Fermi-gas prediction, with  $T = \sqrt{11.3(E^*/A)}$  MeV. Symbols are the same as in Fig. 2.

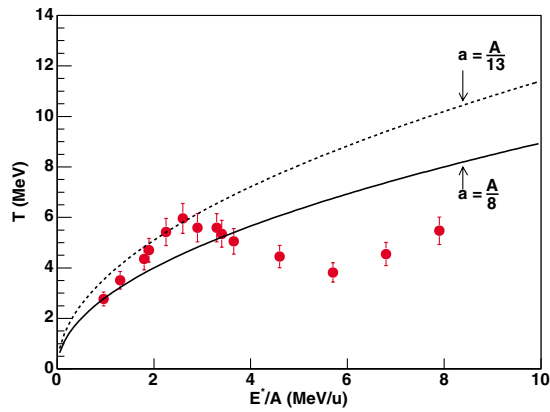


FIG. 4 (color online). Corrected temperature versus excitation energy per nucleon for the data of Fig. 2. Circles show the density-corrected temperature points for the data. The solid and dashed lines show the Fermi-gas behavior for  $K = 8$  MeV and  $K = 15.2$  MeV with no density dependence.

2.5 MeV/A (which is suggested by the lower-energy data in the referenced figure) and a constant value of  $K = 15.2$  MeV above  $E^*/A = 2.5$  MeV.

To evaluate  $\epsilon_{th}$ , we first calculated the binding energies per nucleon,  $\epsilon_{BE}$ , at the different derived densities using the liquid drop mass formula of Myers and Swiatecki [31]. The surface term was scaled as the bulk term and the Coulomb term corrected for expansion. The binding energy changes evaluated in this way show a near parabolic dependence on density similar to that employed in the expanding emitting source model of Friedman [4]. However, the absolute values are slightly lower. Using these values, the thermal excitation energy per nucleon becomes  $\epsilon_{th} = E^*/A - \Delta\epsilon_{BE}$ , where  $\epsilon_{BE}$  is the difference between the binding energy per nucleon at normal density and that at the derived density. At  $E^*/A = 7.9$  MeV we estimate  $\epsilon_{th} = 4.4$  MeV.

These methods are used to evaluate  $K_0$  and  $\epsilon_{th}$  for use in Eq. (1). The resulting temperatures are plotted against the calorimetric excitation energies in Fig. 4. The general trend in Fig. 4 is similar to that seen in the previous figure, but this method of analysis leads to a dip in the “plateau region.” This dip arises from the mismatch created by the abrupt slope change of the derived densities near  $E^*/A = 5$  MeV compared with the assumed parabolic, monotonically increasing expansion-energy corrections of the model used to derive  $T$  from the densities.

In summary, breakup densities have been deduced from the systematic trends in the Coulomb observables for IMF spectra produced in light-ion-induced reactions on  $^{197}\text{Au}$ . The extracted average densities are consistent with  $\langle\rho/\rho_0\rangle \sim 1.0$  up to  $E^*/A \sim 2$  MeV but then gradually decrease, consistent with the models of Friedman [4] and Sobotka *et al.* [5]. Above  $E^*/A \sim 5$  MeV, the obtained constant value of  $\rho/\rho_0 \sim 0.3$  is intermediate between experimentally based values of  $\rho/\rho_0 \sim 0.4$  [11] and  $\rho/\rho_0 \sim 0.2$  [32], and is consistent with the breakup

density assumed in the multifragmentation models of Refs. [1–3]. Thus, the evolution of nuclear density as a function of excitation energy and caloric-curve behavior can be accounted for by a mechanism in which the fragmentation process is driven by thermal pressure and Coulomb effects. Alternatively, Sobotka *et al.* have recently employed the concept of a metastable mononucleus, coupled with changing effective mass, to produce a decrease in density and a caloric curve with a plateau similar to that found in both the present work and the caloric curves based in isotope-ratio temperatures [11].

The authors wish to acknowledge their collaborators on IUCF experiment E304, NSCL experiment E88036, and LNS Saclay experiment E228. We also thank L. G. Sobotka and R. T. de Souza for stimulating discussions regarding this work and Sylvie Hudan and Lai Wan Woo for assistance with the figures. The present research was supported by the U.S. Department of Energy and the Robert A. Welch Foundation.

- 
- [1] D. H. E. Gross, Rep. Prog. Phys. **53**, 1122 (1990).
  - [2] D. Durand, Nucl. Phys. **A541**, 266 (1992).
  - [3] A. S. Botvina *et al.*, Phys. Rev. C **59**, 3444 (1999).
  - [4] W. A. Friedman, Phys. Rev. C **42**, 667 (1990).
  - [5] L. G. Sobotka *et al.*, Phys. Rev. Lett. **93**, 132702 (2004).
  - [6] L. Beaulieu, Phys. Rev. Lett. **84**, 5971 (2000).
  - [7] J. Pochodzalla, Phys. Rev. Lett. **75**, 1040 (1995).
  - [8] J. M. Poskanzer *et al.*, Phys. Rev. C **4**, 1979 (1971).
  - [9] N. T. Porile, Phys. Rev. C **39**, 1914 (1989).
  - [10] S. J. Yennello *et al.*, Phys. Rev. C **41**, 79 (1990).
  - [11] J. B. Natowitz *et al.*, Phys. Rev. C **66**, 031601(R) (2002).
  - [12] J. Albergo, Nuovo Cimento Soc. Ital. Fis. **89A**, 1 (1985).
  - [13] J. Zhang *et al.*, Phys. Rev. C **56**, 1918 (1997).
  - [14] J. L. Wile *et al.*, Phys. Rev. C **45**, 2300 (1992).
  - [15] D. S. Bracken *et al.*, Phys. Rev. C **69**, 034612 (2004).
  - [16] K. Kwiatkowski *et al.*, Phys. Lett. B **423**, 21 (1998).
  - [17] T. Lefort *et al.*, Phys. Rev. C **64**, 064603 (2001).
  - [18] G. D. Westfall *et al.*, Phys. Rev. C **17**, 1368 (1978).
  - [19] L. G. Moretto, Nucl. Phys. **A247**, 211 (1975).
  - [20] K. Kwiatkowski *et al.*, Phys. Lett. B **171**, 41 (1986).
  - [21] V. E. Viola *et al.*, Phys. Rev. C **31**, 1550 (1985).
  - [22] L. Beaulieu *et al.*, Phys. Rev. C **64**, 064604 (2001).
  - [23] A. Ruangma *et al.*, Phys. Rev. C **66**, 044603 (2002).
  - [24] C. B. Das *et al.*, Phys. Rev. C **66**, 044602 (2002).
  - [25] P. Bonche *et al.*, Nucl. Phys. **A427**, 278 (1984); P. Bonche *et al.*, Nucl. Phys. **A436**, 265 (1986).
  - [26] J. B. Natowitz *et al.*, Phys. Rev. C **65**, 034618 (2002).
  - [27] R. Hasse and P. Schuck, Phys. Lett. B **179**, 313 (1986).
  - [28] P. F. Bortignon and C. H. Dasso, Phys. Lett. B **189**, 381 (1987).
  - [29] S. Shlomo and J. B. Natowitz, Phys. Lett. B **252**, 187 (1990); S. Shlomo and J. B. Natowitz, Phys. Rev. C **44**, 2878 (1991).
  - [30] E. J. Moniz *et al.*, Phys. Rev. Lett. **26**, 445 (1971).
  - [31] W. D. Myers and W. J. Swiatecki, Phys. Rev. C **57**, 3020 (1998).
  - [32] G. Verde, Phys. Rev. C **67**, 034606 (2003); (private communication).